Human Basal Cell Carcinoma Is Associated with Foxp3$^+$ T cells in a Th2 Dominant Microenvironment

Helen G. Kaporis[1], Emma Guttman-Yassky[1], Michelle A. Lowes[1], Asifa S. Haider[1], Judilyn Fuentes-Duculan[1], Kamruz Darabi[1], Julia Whynot-Ertelt[1], Artemis Khatcherian[1], Irma Cardinale[1], Inna Novitskaya[1], James G. Krueger[1] and John A. Carucci[2]

Basal cell carcinoma (BCC), the most common human cancer, undergoes spontaneous regression in certain circumstances, which is potentially immune-mediated. To understand the immune response surrounding BCCs, we characterized the genomic, protein, and cellular microenvironment associated with BCC in comparison to normal skin. Our results demonstrated the following: (1) CD4$^+$CD25$^+$Foxp3$^+$ surround epithelial tumor aggregates; (2) Immature dendritic cells (DCs) were abundant in the tumor microenvironment; (3) BCC showed increased expression of IL-4, IL-10, and CCL22 and increased expression of interferon-associated genes (IFI27, IRF1, IRF7, and G1P2) and IL-12/23, gene indicating a Th2 dominant microenvironment. Our findings suggest a dynamic state within the immune microenvironment associated with BCC. The finding of phenotypic T regs, in conjunction with immature DCs and Th2 cytokines, suggests an attenuated state of immunity to human BCC. In contrast, abundant CD8$^+$ T cells, an interferon signal, and IL-12/23 suggest partial host antitumor response. A better understanding of these opposing forces within the immune microenvironment may facilitate development of more potent immune-based treatment for BCC and other human carcinomas.

Journal of Investigative Dermatology (2007) **127,** 2391–2398; doi:10.1038/sj.jid.5700884; published online 17 May 2007

INTRODUCTION

Basal cell carcinoma (BCC) is the most common human cancer affecting nearly one million patients in the United States annually. It is usually characterized by slow growth and low metastatic potential. However, if untreated or incompletely treated, BCC results in massive local tissue damage. Although the mainstay of therapy is surgical removal with tumor-free margins, immune response modifiers, including IFNα (Tucker *et al.*, 2006) and imiquimod (Geisse *et al.*, 2004), have been used with varying degrees of success (ranging between 75 and 96%). Immune responses within the skin may be important in limiting the spread of cutaneous tumors, and harnessing the potential for specific antitumor immunity may be key in optimizing non-surgical approaches to BCC therapy.

Excised BCCs display an inflammatory response with cytotoxic T cells and dendritic cells (DCs) present (Azizi *et al.*, 1987). Local production of cytokines, including IFN-γ, IL-2, IL-10, transforming growth factor-β (TGF-β), and GM-CSF, has been described (Kim *et al.*, 1995; Wong *et al.*, 2000). The brisk inflammatory response coupled with the inability to completely eradicate tumors, suggests a dynamic state where immune stimulatory and immune suppressive forces coexist and compete. With the recent use of immune response modulators augmenting Th1 responses such as topically applied imiquimod to treat BCCs, there is now evidence that the immune system may be activated for successful tumor eradication (Geisse *et al.*, 2004; Wenzel *et al.*, 2005; Tucker *et al.*, 2006). Imiquimod induces IFN-α and Th1 cytokines including IL-12 (Stanley, 2002), results in recruitment of plasmacytoid DCs expressing interferon-associated genes (Urosevic *et al.*, 2005), and induces apoptosis in BCC (Schon *et al.*, 2003). However, there are many aspects of antitumor immunity in BCC that are not fully characterized.

Quantitative analysis, precise localization, and phenotyping of the cells comprising the inflammatory infiltrate within and surrounding BCCs, along with characterization of immune response gene expression, is fundamental in establishing a baseline for designing and evaluating immunotherapy and for determining the effects of immune suppression on tumor behavior. We aimed to quantify, localize, and phenotype the BCCs associated infiltrate and also evaluate the expression of immune response genes in BCC. We have determined the following: (1) CD4$^+$, CD25$^+$FoxP3$^+$ cells (phenotypic T regs) surround BCC; (2) myeloid DCs but no Langerhans cells were associated with BCC; (3) BCC was characterized by a Th2 dominant microenvironment.

[1]*Laboratory for Investigative Dermatology, Rockefeller University, New York, New York, USA and* [2]*Section of Mohs Micrographic and Dermatologic Surgery, Weill Medical College of Cornell, New York, New York, USA*

Correspondence: Dr John A. Carucci, Department of Dermatology, Cornell University, 525 East 68th St, Starr 326, New York, New York 10021, USA. E-mail: jac2015@med.cornell.edu

Abbreviations: BCC, Basal cell carcinoma; DCs, dendritic cells; HARP, human acidic ribosomal protein; JTD, juxtatumoral dermis; NLPD, non-lesional papillary dermis; NPD, normal papillary dermis; RT, reverse transcriptase; T, tumor

Received 7 September 2006; revised 30 January 2007; accepted 20 February 2007; published online 17 May 2007

RESULTS

Localization and characterization of the immune microenvironment of BCC

We set out to define and precisely localize the cells that make up the microenvironment surrounding BCC (Figure S1). The regions examined within BCC samples were designated tumor (T) and juxtatumoral dermis (JTD). Skin immediately adjacent to tumors was analyzed, with regions designated as non-lesional papillary dermis (NLPD) and non-lesional epidermis (Figure S1). Normal skin from non-exposed areas of healthy volunteers was designated normal epidermis and normal papillary dermis (NPD). As BCC develops from basal epidermis, we compared infiltrating leukocytes in normal skin *versus* adjacent skin and tumor. We also compared NPD *versus* NLPD and, JTD based on the structural similarities between these regions.

The inflammatory infiltrate associated with BCCs was characterized by significantly higher numbers of $CD8^+$ cells with lower numbers of Langerhans cells

Relatively, few $CD3^+$ cells were found in NPD with significantly higher numbers being demonstrated in NLPD ($P<0.01$; Figure 1) and JTD ($P<0.001$; Figure 1). This was mirrored by $CD8^+$ cells, which were increased in NLPD *versus* NPD and JTD (both $P<0.04$; Figure 1). DCs, while capable of penetrating tumor nests, were predominantly localized to JTD. The numbers of $CD1a^+$ cells (Langerhans cells) were significantly higher in the normal epidermis *versus* the epidermis overlying the non-tumor bearing dermis from BCC patients ($P<0.0004$; Figure 1). The numbers of Langerhans cells were significantly lower in epithelial tumor aggregates *versus* the epidermis overlying non-tumor bearing dermis ($P<0.00001$). In contrast to T lymphocytes, $CD11c^+$ and $CD1b/c^+$ cells showed relatively little change in JTD when compared with NLPD (Figure 1). $CD40^+$, $CD83^+$, and DC $LAMP^+$ cells were absent in BCC (data not shown) indicating a lack of mature DCs. Staining for CD4 on tissue sections was not performed, as that marker appears on DCs as well T-helper cells.

Phenotypic regulatory T cells surround BCC aggregates

We found that $CD3^+$ and $CD8^+$ T cells predominantly aggregate in JTD. A progressive increase in T cells was noticed within the respective dermal regions from NPD to NLPD to JTD (Figure 1). To determine whether regulatory T cells (T regs) might be associated with BCC, $Foxp3^+$ cells were quantified by immunohistochemistry (Figure 2a). There were significantly increased numbers of $Foxp3^+$ in the JTD compared with NLPD ($P<0.01$) and NPD ($P<0.0001$). Triple label IF confirmed the presence of $CD4^+CD25^+$Fox $P3^+$ cells, which are phenotypically identical to regulatory T cells (Figure 2b). Double label immunofluorescence was performed to confirm that these $Foxp3^+$ cells also expressed CD3 (Figure 2c). Interestingly, $CD3^+$ and $CD8^+$ cells were present not only in the JTD, but also in direct contact with the tumor margins forming a ''pseudocapsule'' around the BCC (Figure 2d). $Foxp3^+$ T cells were detected in the pseudocapsular margins as well as penetrating the tumor nodules.

Genomic analysis of BCC microenvironment

We performed genomic analysis of BCC, adjacent non-tumor bearing skin, and normal skin to assess differential expression of immune response genes in BCC (Figure 3). We included normal skin recognizing that the effects of UV exposure might influence non-tumor bearing skin adjacent to excised BCC. Microarray data showed increased expression of interferon-associated genes, including IFI27, IRF1, IRF7 and G1P2 in BCC *versus* normal skin. Angiogenesis-associated genes, including CXCR4 and IL-1β, were upregulated in BCC *versus* normal skin, whereas IL-6 and CXCL2 were upregulated in non-tumor bearing skin adjacent to BCC compared with normal skin. Expression of CXCL9, CCL2, CCL20, IL-4 receptor, and CD3D were increased in BCC *versus* normal skin. Expression of CCL27 (CTACK) was highest in normal skin and higher in peritumoral skin compared with BCC. Data are summarized in Figure 3.

Differential expression of CXCL9, CXCL12, CCL15, CCL27, IL-1β, and IL-6 was confirmed by reverse transcriptase-PCR (RT-PCR) (Figure 4). In addition, RT-PCR analysis showed increased expression of IL-4, IL-10, IL-CCL22, P19, and P40 subunits of IL-23 were in BCC *versus* normal skin. Tumor contained lower levels of IFN-γ, TGF-β, and IL-17 compared with normal skin.

DISCUSSION

We have quantified and localized DCs and $Foxp3^+$T cells associated with BCC, and we have also performed comparative genomic analysis of immune response genes in BCC *versus* adjacent non-tumor bearing and normal skin. Several findings stand out: (1) $CD4^+CD25^+$Fox $P3^+$ (phenotypic T regs) surround epithelial aggregates of BCC; (2) BCC-associated myeloid DCs are primarily immature; (3) there is increased expression of IL-4, IL-10, CCL22, which favors a Th2 environment and increased expression of interferon-associated genes (IFI27, IRF1, IRF7 and G1P2) favoring Th1.

Current theories of carcinogenesis are evolving to explain how cancer proceeds despite ''immunosurveillance'' (Zitvogel *et al.*, 2006). Although rarely completely effective, the immune system is able to recognize and destroy cancer cells. T cells, DCs, and their products appear to be involved in this antitumor host response. However, the cancer cells may develop mechanisms to subvert these effects. The end result of this balance between host antitumor responses and tumor survival tactics will either lead to tumor eradication (regression) or tumor growth. The data in our paper support this concept. Interferon-associated genes represent an ongoing antitumor response; T regs, immature DCs, and Th2 genes are all features that would allow tumor survival.

T regs are recently described as T cells that appear to control immune responses in an antigen-specific manner (Rutella and Lemoli, 2004). Mediators responsible for T reg development include IL-10 and TGF-β (Rutella and Lemoli, 2004). We found an upregulation of IL-10 but decreased TGF-β mRNA. This combination may still be sufficient to induce T regs, and the genomic levels of these cytokines may not correlate directly with protein expression. In addition, the chemokine responsible for T reg chemotaxis, CCL22, is also

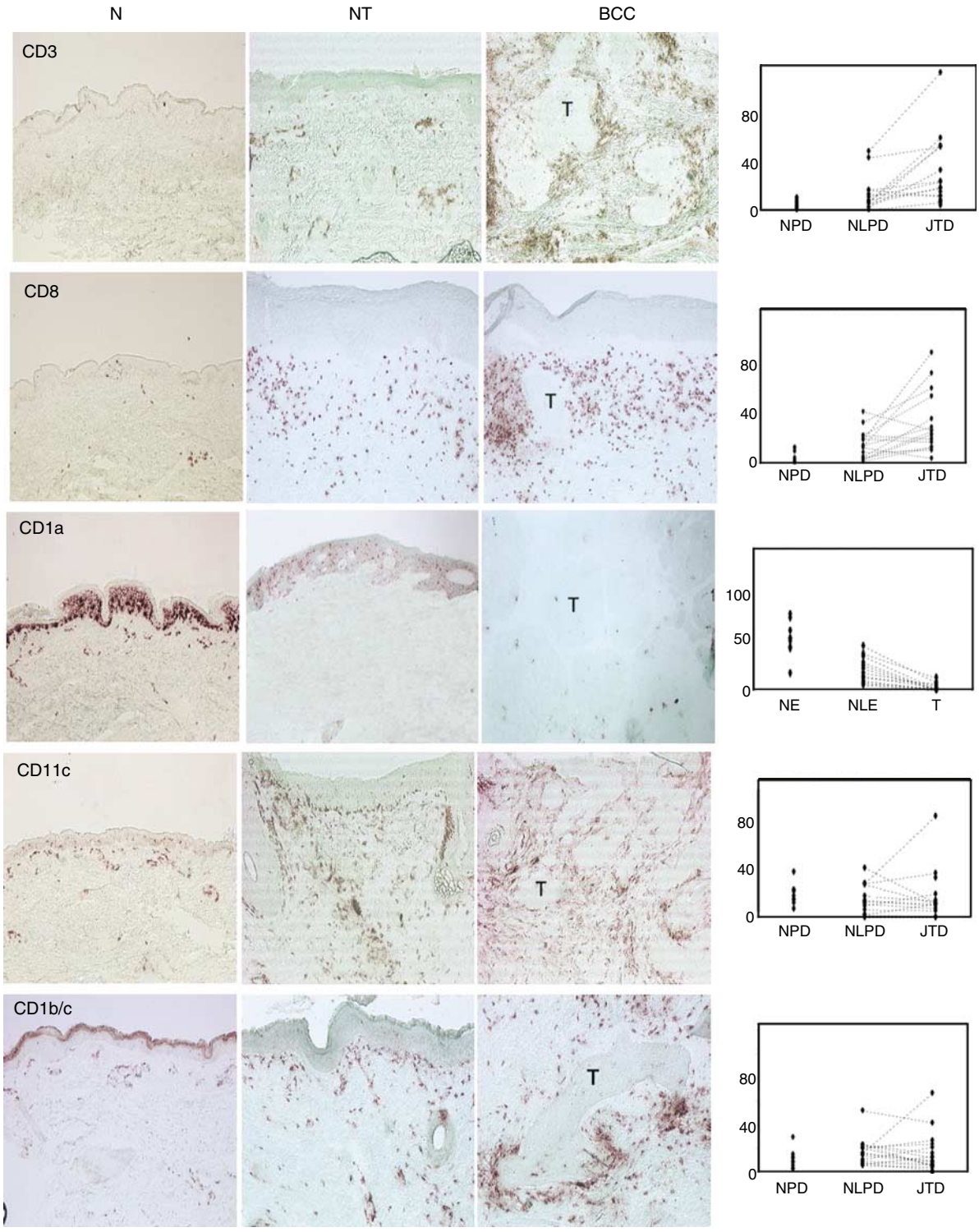

Figure 1. Characterization of the microenvironment associated with BCC. Cell counts showed increased numbers of $CD3^+$ and $CD8^+$ T cells and decreased numbers of $CD1a^+$ Langerhans cells associated with BCC. Numbers of $CD1b/c^+$ and $CD11c^+$ were unchanged in non-lesional dermis *versus* JTD.

increased in BCC (Curiel *et al.*, 2004; Lee *et al.*, 2005; Yang *et al.*, 2006), suggesting a mechanism for T reg localization in peri-tumoral areas. T regs appear to control autoimmunity (Rutella and Lemoli, 2004), and may also suppress antitumor responses (Beyer and Schultze, 2006; Beyer *et al.*, 2006). $CD4^+CD25^+Foxp3^+$ T regs from ovarian carcinoma patients suppressed tumor-specific T-cell immunity (Garcia-Castro *et al.*, 2001; Curiel *et al.*, 2004). Studies have also correlated higher T-reg cell frequencies in gastric carcinoma patients with poorer prognosis and decreased survival rates

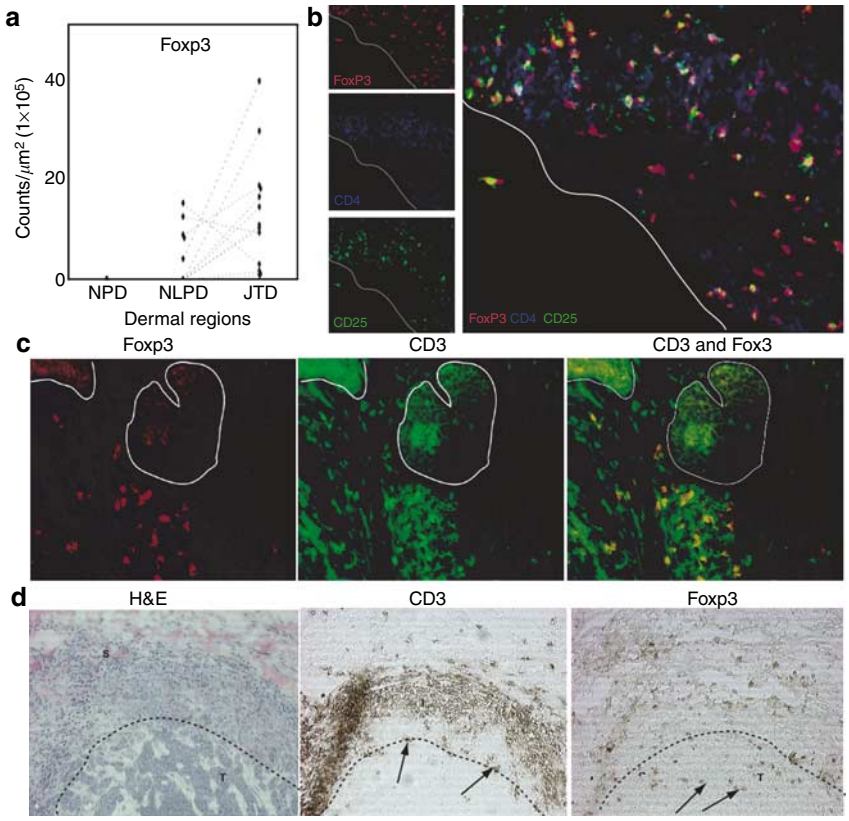

Figure 2. Phenotypic regulatory T cells are associated with human BCC. (**a**) Inflammatory cells form a ''pseudocapsule'' around the tumor nodule. Infiltrating mononuclear cells (arrows). The interface of tumor (T)/stroma (S) (dashed lines). FoxP3$^+$ cells were present in the ''pseudocapsule'' surrounding BCC. (**b**) Double label immunofluorescence confirmed that FoxP3$^+$ cells expressed CD3. (**c**) Triple label immunofluorescence showing CD4$^+$CD25$^+$Foxp3$^+$ cells associated with BCC. (**d**) Cell counts show increased numbers of Foxp3$^+$ cells in JTD *versus* NLPD *versus* normal skin.

(Beyer and Schultze, 2006). In BCCs, the presence of Foxp3$^+$ cells surrounding the tumor nodules may attenuate the function of DCs and cytotoxic T cells.

Mechanisms by which T regs suppress immunity *in vivo* are poorly understood and may involve antigen-presenting cells. T regs may impair DC maturation or suppress expression of DC co-stimulatory molecules, and IL-10 may be responsible for both these effects (Nestle *et al.*, 1997; Houot *et al.*, 2006). This may be consistent with our findings, which include increased IL-10 and immature DCs (CD40$^-$, CD86$^-$, CD83$^-$, and DC LAMP). In addition, UV may also induce IL-10 (Enk *et al.*, 1995), which could contribute to this effect. BCCs occur in sun-exposed areas, and thus the potential effects of UV exposure on local DCs may also be additive.

It is possible that immature DCs are involved in attenuating the immune response to BCC, and in our studies, the BCC microenvironment was associated with high the number of immature DCs. Immature DCs play a role in the induction of peripheral T-cell tolerance (Steinman *et al.*, 2003; Banerjee *et al.*, 2006). Tolerogenic DCs with a distinctive IL-10$^+$ IL-12$^-$ cytokine production profile have been described (Rutella and Lemoli, 2004; Rutella *et al.*, 2006a,). A regulatory DC subset, which secreted high levels of IL-10 and suppressed T-cell proliferation *in vitro* and *in vivo* has also been described (Tang *et al.*, 2006). In addition, immature DCs may contribute to tumor proliferation directly as immature DCs support growth of human cutaneous T-cell lymphoma cells for extended periods (Berger *et al.*, 2002).

Another factor that could contribute to an immunosuppressive environment is the increased expression of Th2 cytokines. Although others have found a similar Th2 cytokine profile in BCC (Kim *et al.*, 1995), we confirm an increase in IL-4, IL-10, but extend this to include CCL22 (MDC), which may be chemotactic for Th2 cells (Vulcano *et al.*, 2001).

In contrast to these potential tumor-permissive mechanisms discussed above, there may be concurrent immune responses directed toward tumor eradication. Trafficking of CD8$^+$ cells to the JTD supports the potential for a specific adaptive antitumor response. We found increased expression of interferon-associated genes IFI27, IRF1, IRF7, and G1P2. Other important cytokines that may be responsible for DC activation were also increased in BCCs. P19 (a component of IL-23) and p40 (shared subunit of IL-12 and IL-23) were both elevated in BCC. IL-23 can enhance the proliferation of memory T cells and production of IFN-γ from activated T cells, and can induce antitumor effects *in vitro* (Shan *et al.*, 2004, 2006). Similarly, IL-12 may activate DCs and mediate Th1 antitumor immunity (Colombo and Trinchieri, 2002). This is consistent with induction of IL-12 among other

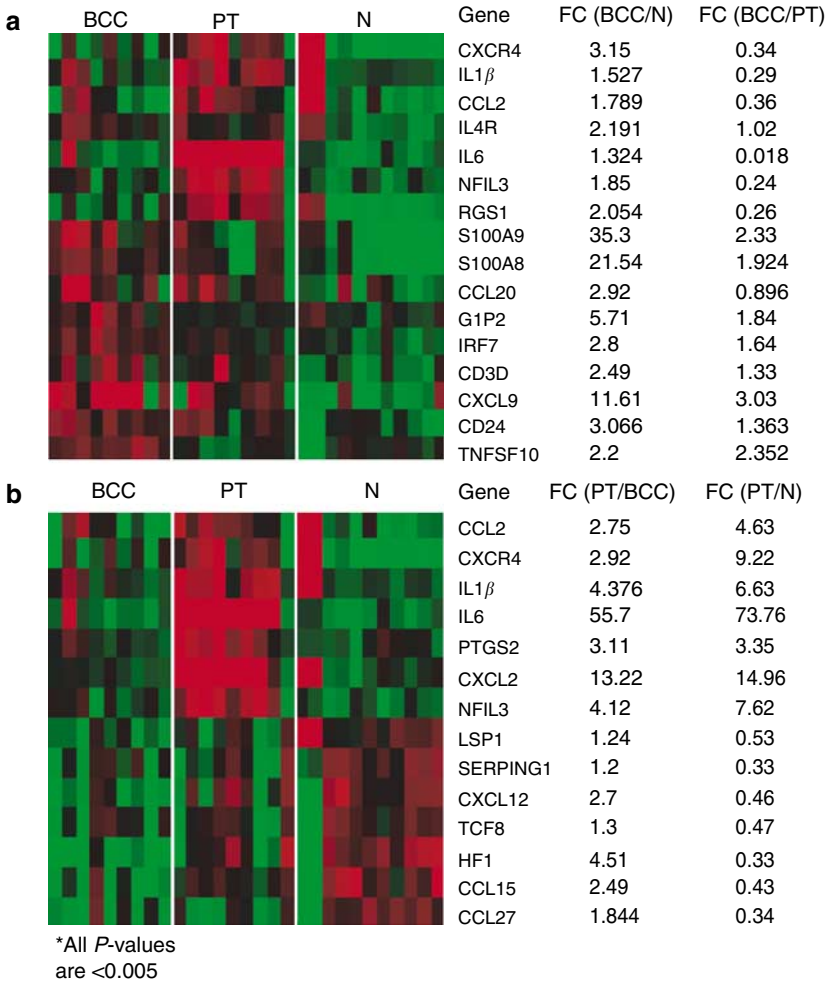

Figure 3. Expression profiling for immune response genes in BCC, adjacent non-tumor bearing skin, and normal skin. Gene array analysis of mRNA from nine basal cell carcinoma (BCC), nine site-matched, patient-matched, non-tumor bearing skin (PT), and 10 normal skin samples (N). mRNA was hybridized to individual oligonucleotide arrays containing ~12,000 human genes (HG-U95A/Av2 chips). Heat map shows unsupervised, hierarchical clustering for gene expression differences that are statistically significant ($P<0.05$, after correction for multiplicity). Fold changes (FC) shown for BCC *versus* normal (BCC/N), BCC *versus* adjacent non-tumor bearing skin (BCC/PT), (adjacent non-tumor bearing skin *vs* BCC (PT/BCC), and adjacent non tumor bearing skin *versus* normal skin (PT/N). (**a**) Genes differentially expressed in BCC *versus* peritumoral skin or normal skin. (**b**) Genes differentially expressed in peritumoral skin *versus* BCC or normal skin.

cytokines during imiquimod treatment for BCC (Stanley, 2002).

In summary, our studies suggest a dynamic state within the immune microenvironment associated with BCC. The finding of phenotypic T regs in conjunction with immature DCs and Th2 cytokines suggests an attenuated state of immunity to human BCC. In contrast, abundant $CD8^+$ T cells, an interferon signal, and IL-12/23 suggest partial host antitumor response. Further understanding of the interplay between these forces may facilitate the development of rationally based immune therapy for BCC and other human skin cancers.

MATERIALS AND METHODS

Institutional Review Board approval was obtained before enrolling patients to participate in this study. Informed consent was obtained from patients before their participation, and the study was performed with strict adherence to the Declaration of Helsinki Principles.

Samples used in study *For IHC*

Twenty nodular BCC samples were obtained during Mohs micrographic surgery. Tumors were obtained from head and neck (11/20), trunk (2/20), and extremities (7/20), respectively. Additionally, 10 normal specimens were obtained via 3-mm punch biopsies from non-sun exposed areas of patients without skin tumor.

For Microarray and RT-PCR

Ten paired samples of tumor and site-matched normal skin were obtained during surgery. Site-matched normal skin was obtained from site-matched uninvolved skin at the time of repair after clear margins were achieved. Mean age of patients with BCC in this study was 73 years (range: 46–83). Mean tumor size 1.0×0.8 cm. Average final tumor defect after clearing tumors was 1.9×1.8 cm. All tumors with one exception were located on sun-exposed areas. For genomic studies on normal skin, 10 normal specimens were obtained via

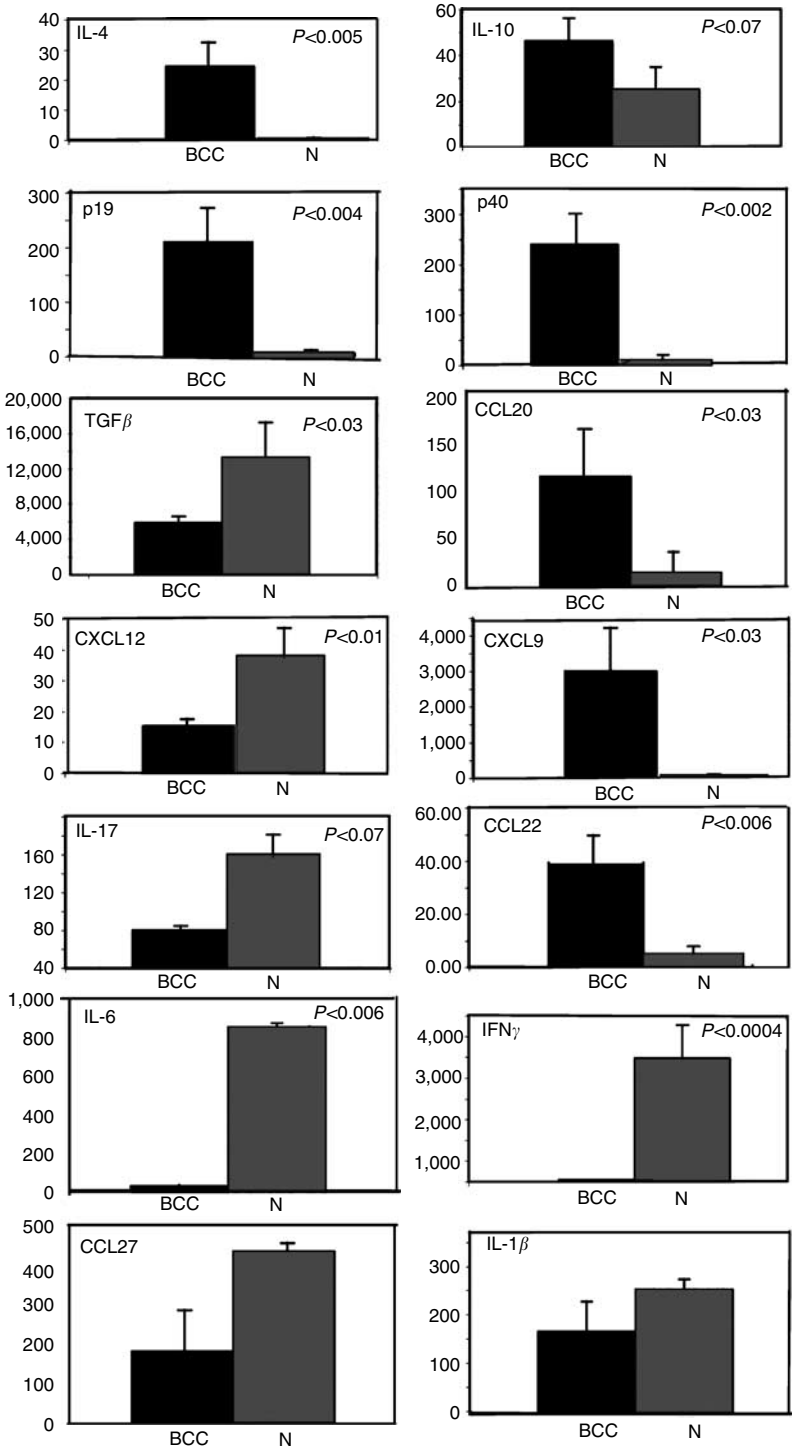

Figure 4. Real time RT-PCR analysis of selected genes in BCC and normal skin. Mean values of gene expression for selected genes are graphically represented after normalization of expression using gene to HARP mRNA. mRNA was analyzed from BCC specimens (BCC) and normal skin (N) ($n=9$ for each). IL-4, IL-10, P19, P40, CXCL9, and CCL22 were increased in BCC. IFNγ, TGF-β, IL-6, IL1β, IL-17, CXCL12, and CCL27 were decreased in BCC.

3-mm punch biopsies from non-sun exposed areas of patients without skin cancer.

Immunohistochemistry

Frozen tissue sections were stained with hematoxylin (Fisher, Fair Lawn, NJ) and eosin (Shandon, Pittsburgh, PA) and with purified mouse anti-human monoclonal antibodies to CD1b/c (Biosource, Camarillo, CA; diluted 1/100), CD11c, CD1a, CD8, CD3, CD83, CD40, CD16, CD25, CD40, and HLADR (BD Pharmingen, San Diego, CA; all diluted 1/100 except CD40 (1/50) and HLADR (1/200), Langerin, DC-LAMP (Immunotech, Cedex, France; (1/50), CD86 (Genetex, San Antonio, TX; diluted 1/100), CTACK/CCL27

(R&D Systems, Minneapolis, MN; diluted 1/500), Foxp3 (Abcam, Cambridge, MA diluted 1/40). Biotin-labeled horse anti-mouse antibody (Vector Laboratories, Burlingame, CA) was amplified with avidin–biotin complex (Vector Laboratories) and developed with chromogen 3-amino-9-ethylcarbazole (Sigma Aldrich, St Louis, MO). Counterstaining was performed with light green (Sigma Aldrich). Appropriate isotype controls were performed with each immunohistochemistry experiment.

Image analysis

Tumor-bearing skin and non-tumor bearing skin adjacent to excised tumor, and normal skin from volunteers were evaluated for the expression of a wide panel of surface markers by immunohistochemistry and immunofluorescence. The regions examined within BCC samples were designated tumor (T), JTD, NLPD and non-lesional epidermis. The regions examined within normal skin included normal epidermis and NPD. NPD, NLPD, and JTD were compared in this study based on the structural similarities between these regions. Positive cells were counted manually, and area measures were computed by computer-assisted image analysis, National Institutes of Health software (NIH IMAGE 6.1). Cell counts per μm^2 were determined within normal and non-lesional epidermis, papillary dermis (100 μm deep to the epidermis), BCC epithelial aggregates, and JTD (100 μm circumferential to tumor). In all cases, tumor sections with the most brisk response were selected for analysis.

Statistical analysis

Statistical comparisons of cell counts were performed using a two-tailed, Student's *t*-test, with $P<0.05$ considered significant.

RNA preparation

The total RNA was processed as described previously (Haider *et al.*, 2006). Briefly, the microarrays used for this study were U95A-set GeneChip probe arrays (Affymetrix Inc., Santa Clara, CA) containing probe sets of approximately 12,000 genes. The labeled target was fragmented, and hybridized to probe arrays as described previously (Zhou *et al.*, 2003). Briefly, total RNA was extracted from tissues frozen in liquid nitrogen using the RNeasy Mini Kit (Qiagen, Valencia, CA). DNA was removed with on-column DNAse digestion by Qiagen RNAse-free DNAse Set. Total RNA ($\sim$4 μg) was reverse-transcribed, amplified, and labeled. mRNA was isolated and converted to double-strand cDNA and then to biotinylated cRNA (BioArray High Yield RNA Transcription Labeling Kit; Enzo Biochem Inc., Farmingdale, NY). After fragmentation and quality confirmation with Affymetrix Test-3 Array, 15 μg of the biotinylated cRNA were hybridized to Affymetrix Human Genome U95A GeneChips (12,000 probe sets) (Affymetrix Inc.). The chips were washed, stained with streptavidin–phycoerythrin and, scanned (HP GeneArray Scanner, Hewlett–Packard Company, Palo Alto, CA). On each chip, the human housekeeping genes β-actin and GAPDH served as controls. Suite 5.0 software normalized the expression level values using these controls. Chips with 3′ to 5′ ratios for GAPDH less than 3 and scaling factor within threefold of each other were compared for the study.

Microarray analysis

To obtain a list of biologically most interesting genes used in this study, multiple statistical analyses were performed. Statistical comparisons of expression levels pairwise between each condition (BCC, NT, and N) were performed by using Gene Spring Software. On the basis of full data set, paired *t*-tests were performed to assess the interesting genes for the distinction. Owing to the multiple testing problems encountered in the analysis of microarray data, we chose to declare those genes with a false discovery rate of at most 5% as having a significant effect. In this study, genes that passed the Benjamini–Hochberg criterion were considered. A list of significantly regulated immune response genes (Benjamini–Hochberg false discovery rate 5%) is presented as up- or downregulated greater than twofold based on the average of eight patients (BCC *vs* N, BCC *vs* NT).

Expression changes with real-time RT-PCR analysis of tissue mRNA gene expression

TaqMan RT-PCR assays were generated with the Assay on Demand primers and probes for P19, P40, IL-1β, IL-6, IL-4, IL-10, IL-17, IFN-γ, TGF-β, CCL 20 (MIP3α), CCL27 (CTACK), CXCL12, CXCL9, and CCL22 designed by Applied Biosystem (Foster City, CA). The RT-PCR reaction was performed using EZ PCR Core Reagents (Applied Biosystems) according to the manufacturer's directions. The samples were amplified and quantified on an Applied Biosystems PRISM 7700 using the following thermal cycler conditions: 2 minutes at 50°C; 30 minutes at 60°C; 5 minutes at 95°C; and 40 cycles of 15 seconds at 95°C followed by 60 seconds at 60°C. The human acidic ribosomal protein (HARP) gene, a housekeeping gene, was used to normalize each sample and each gene. Primer sequences HARP-forward, CGCTGCTGAACATGCT CAA; HARP-reverse, TGTCGAACACCTGCTGGATG; HARP-probe, 6-FAM-TCCCCCTTCTCCTTTGGGCTGG-TAMRA (GenBank accession no. NM-001002) were used. The data were analyzed and samples quantified by the software provided with the Applied Biosystems PRISM 7700 (Sequence Detection Systems, version 1.7).

Statistical analysis

Statistical comparisons of mRNA expression level was performed using a two-tailed, Student's *t*-test, with $P<0.05$ considered significant.

CONFLICT OF INTEREST

These authors state no conflict of interest.

ACKNOWLEDGMENTS

This work was supported in part by the Dermatology Foundation.

SUPPLEMENTARY MATERIAL

Figure S1. Definition of regions within BCC specimens.

REFERENCES

Azizi E, Bucana C, Goldberg L, Kripke ML (1987) Perturbation of epidermal Langerhans cells in basal cell carcinomas. *Am J Dermatopathol* 9:465–73

Banerjee DK, Dhodapkar MV, Matayeva E, Steinman RM, Dhodapkar KM (2006) Expansion of FOXP3 high regulatory T cells by human dendritic cells (DCs) *in vitro* and after injection of cytokine-matured DCs in myeloma patients. *Blood* 108:2655–61

Berger CL, Hanlon D, Kanada D, Dhodapkar M, Lombillo V, Wang N *et al.* (2002) The growth of cutaneous T-cell lymphoma is stimulated by immature dendritic cells. *Blood* 99:2929–39

Beyer M, Kochanek M, Giese T, Endl E, Weihrach MR, Knolle PA *et al.* (2006) *In vivo* peripheral expansion of naive CD4+CD25high FoxP3+ regulatory T cells in patients with multiple myeloma. *Blood* 107:3940–9

Beyer M, Schultze JL (2006) Regulatory T cells in cancer. *Blood* 108:804–11

Colombo MP, Trinchieri G (2002) Interleukin-12 in anti-tumor immunity and immunotherapy. *Cytokine Growth Factor Rev* 13:155–68

Curiel TJ, Coukos G, Zou L, Alvarez X, Cheng P, Mottram P *et al.* (2004) Specific recruitment of regulatory T cells in ovarian carcinoma fosters immune privilege and predicts reduced survival. *Nat Med* 10:942–9

Enk C, Sredni D, Blauvelt A, Katz SI (1995) Induction of IL-10 gene expression in human keratinocytes by UVB exposure *in vivo* and *in vitro*. *J Immunol* 154:4851–6

Garcia-Castro J, Segovia C, Garcia-Sanchez F, Lilllo R, Gomez-Navarro J, Cruriel DT *et al.* (2001) Selective transduction of murine myelomonocytic leukemia cells (WEHI-3B) with regular and RGD-adenoviral vectors. *Mol Ther* 3:70–7

Geisse J, Caro I, Lindholm J, Golitz L, Stampone P, Owens M (2004) Imiquimod 5% cream for the treatment of superficial basal cell carcinoma: results from two phase III, randomized, vehicle-controlled studies. *J Am Acad Dermatol* 50:722–33

Haider AS, Peters SB, Kaporis H, Cardinale I, Fei J, Ott J *et al.* (2006) Genomic analysis defines a cancer-specific gene expression signature for human squamous cell carcinoma and distinguishes malignant hyperproliferation from benign hyperplasia. *J Invest Dermatol* 126:869–81

Houot R, Perrot I, Garcia E, Durand I, Lebecque S *et al.* (2006) Human CD4+CD25high regulatory T cells modulate myeloid but not plasmacytoid dendritic cells activation. *J Immunol* 176:5293–8

Kim J, Modlin RL, Moy RL, Dubinett SM, McHugh T, Nickoloff BJ *et al.* (1995) IL-10 production in cutaneous basal and squamous cell carcinomas. A mechanism for evading the local T cell immune response. *J Immunol* 155:2240–7

Lee I, Wang L, Wells AD, Dorf ME, Ozkaynak E, Hancock WW (2005) Recruitment of Foxp3+ T regulatory cells mediating allograft tolerance depends on the CCR4 chemokine receptor. *J Exp Med* 201:1037–44

Nestle FO, Burg G, Fah J, wrone-Smth T, Nickoloff BJ (1997) Human sunlight-induced basal-cell-carcinoma-associated dendritic cells are deficient in T cell co-stimulatory molecules and are impaired as antigen-presenting cells. *Am J Pathol* 150:641–51

Rutella S, Bonanno G, Procoli A, Mariotti A, de Ritis DG, Curti A *et al.* (2006a) Hepatocyte growth factor favors monocyte differentiation into regulatory interleukin (IL)-10++IL-12low/neg accessory cells with dendritic-cell features. *Blood* 108:218–27

Rutella S, Danese S, Leone G (2006b) Tolerogenic dendritic cells: cytokine modulation comes of age. *Blood* 108:1435–40

Rutella S, Lemoli RM (2004) Regulatory T cells and tolerogenic dendritic cells: from basic biology to clinical applications. *Immunol Lett* 94(1–2):11–26

Schon M, Bong AB, Drewniok C, Herz J, Geilen CC, Reifenberger KJ *et al.* (2003) Tumor-selective induction of apoptosis and the small-molecule immune response modifier imiquimod. *J Natl Cancer Inst* 95:1138–49

Shan B, Yu L, Shimozato O, Li Q, Tagawa M (2004) Expression of interleukin-21 and -23 in human esophageal tumors produced antitumor effects in nude mice. *Anticancer Res* 24:79–82

Shan BE, Hao JS, Li QX, Tagawa M (2006) Antitumor activity and immune enhancement of murine interleukin-23 expressed in murine colon carcinoma cells. *Cell Mol Immunol* 3:47–52

Stanley MA (2002) Imiquimod and the imidazoquinolones: mechanism of action and therapeutic potential. *Clin Exp Dermatol* 27:571–7

Steinman RM, Granelli-Piperno AG, Pope M, Trumpfeller C, Ignatius R, Arrode G *et al.* (2003) The interaction of immunodeficiency viruses with dendritic cells. *Curr Top Microbiol Immunol* 276:1–30

Tang H, Guo Z, Zhang M, Wang J, Chen G, Cao X (2006) Endothelial stroma programs hematopoietic stem cells to differentiate into regulatory dendritic cells through IL-10. *Blood* 108:1189–97

Tucker SB, Polasek JW, Perri AJ, Goldsmith EA (2006) Long-term follow-up of basal cell carcinomas treated with perilesional interferon alfa 2b as monotherapy. *J Am Acad Dermatol* 54:1033–8

Urosevic MR, Dummer R, Conrad C, Beyeler M, Laine E, Burg G (2005) Disease-independent skin recruitment and activation of plasmacytoid predendritic cells following imiquimod treatment. *J Natl Cancer Inst* 97:1143–53

Vulcano M, Albanesi C, Stoppacciaro A, Bagnati R, D'Amico G, Struyf S *et al.* (2001) Dendritic cells as a major source of macrophage-derived chemokine/CCL22 *in vitro* and *in vivo*. *Eur J Immunol* 31:812–22

Wenzel J, Uerlich M, Haller O, Beiber T, Tueting T (2005) Enhanced type I interferon signaling and recruitment of chemokine receptor CXCR3-expressing lymphocytes into the skin following treatment with the TLR7-agonist imiquimod. *J Cutan Pathol* 32:257–62

Wong DA, Bishop GA, Lowes MA, Cooke B, Barneston RS, Halliday GM (2000) Cytokine profiles in spontaneously regressing basal cell carcinomas. *Br J Dermatol* 143:91–8

Yang ZZ, Novak AJ, Stenson MJ, Witzig TE, Ansell SM (2006) Intratumoral CD4+CD25+ regulatory T-cell-mediated suppression of infiltrating CD4+ T cells in B-cell non-Hodgkin lymphoma. *Blood* 107:3639–46

Zhou X, Krueger JG, Kao MC, Lee E, Du F, Menter A *et al.* (2003) Novel mechanisms of T-cell and dendritic cell activation revealed by profiling of psoriasis on the 63,100-element oligonucleotide array. *Physiol Genomics* 13:69–78

Zitvogel L, Tesniere A, Kroemer G (2006) Cancer despite immunosurveillance: immunoselection and immunosubversion. *Nat Rev Immunol* 6:715–27